LETTER

Hard ferromagnetic van-der-Waals metal $(Fe,Co)_3GeTe_2$: a new platform for the study of low-dimensional magnetic quantum criticality

To cite this article: Inho Hwang *et al* 2019 *J. Phys.: Condens. Matter* **31** 50LT01

View the article online for updates and enhancements.

Letter

Hard ferromagnetic van-der-Waals metal (Fe,Co)$_3$GeTe$_2$: a new platform for the study of low-dimensional magnetic quantum criticality

Inho Hwang[1,2], Matthew J Coak[1,2,3], Nahyun Lee[2], Dong-Su Ko[4],
Youngtek Oh[4], Insu Jeon[4], Suhan Son[1,2], Kaixuan Zhang[1,2],
Junghyun Kim[1,2] and Je-Geun Park[1,2]

[1] Department of Physics and Astronomy, Seoul National University, Seoul 08826, Republic of Korea
[2] Center for Correlated Electron System, Institute for Basic Science (IBS), Seoul 08826, Republic of Korea
[3] Department of Physics, University of Warwick, Coventry CV4 7AL, United Kingdom
[4] Samsung Advanced Institute of Technology, Suwon 16678, Republic of Korea

E-mail: jgpark10@snu.ac.kr

CrossMark

Abstract

The widely-studied ferromagnetic van-der-Waals (vdW) metal Fe$_3$GeTe$_2$ has great promise for studies of quantum criticality in the 2D limit, but is limited by a relatively high Curie temperature in excess of 200 K. To help render the quantum critical point achievable in such a system within the reach of practically possible tuning methods, we have grown single crystals of a variant of (Fe,Co)$_3$GeTe$_2$ with useful physical properties for both this purpose and the wider study of low-dimensional magnetism and spin transport. (Fe,Co)$_3$GeTe$_2$ is found through x-ray diffraction and electron microscopy to have an equivalent crystal structure to Fe$_3$GeTe$_2$, with a random distribution of the cobalt dopant sites. It exhibits a sharp ferromagnetic transition at a value below 40 K, a stronger anisotropy and a coercive field ten times larger than that of Fe$_3$GeTe$_2$. The transport properties and specific heat show the electronic properties and strong correlations of Fe$_3$GeTe$_2$ to be near-unchanged in this doped material. We demonstrate that (Fe,Co)$_3$GeTe$_2$ can be cleanly exfoliated down to monolayer thickness. This unprecedented hard metallic vdW ferromagnet is a valuable new addition to the limited range of materials available for the study of 2D magnetism.

Keywords: quantum criticality, van der Waals layered compounds, ferromagnetism

(Some figures may appear in colour only in the online journal)

1. Introduction

How well-known physical concepts change upon reduction of physical dimension from three-dimensions (3D) to 2D and even to 1D has remained a core question in condensed matter physics over the last several decades. Justifying this long scientific endeavor, it has proven to be a fertile ground where one can find new novel physics: a prime example being the topological transition discovered in the 70s by the trio of Berezinskii–Kosterlitz–Thouless [1, 2]. With reduced

dimensionality, quantum fluctuations are intrinsically stronger and sometimes dominant over other energy scales and have long been demonstrated to open up completely new avenues of original physics—including in strengthening unconventional superconductivity pairing.

The recent arrival of a new class of magnetic van-der-Waals (vdW) materials, often called magnetic graphene because of their 2D honeycomb lattice of magnetic elements, is therefore a welcome advancement in the field, with new possibilities and questions [3, 4]. Although there have been numerous attempts towards realizing low-dimensional magnetism, mainly in thin films synthesized by, for instance, pulsed-laser deposition for oxides and sputtering for metals, a big advantage with the new magnetic vdW materials is the elegant simplicity of the Scotch tape method with which one can produce very thin samples and even single atomic layers. For example, it has been demonstrated that both antiferromagnetic and ferromagnetic ordering of the Ising-type can survive down to monolayer thickness, consistent with the theoretical predictions made back in the 1940s by Onsager [5]; examples are $FePS_3$ [6], $Cr_2Ge_2Te_6$ [7], and CrI_3 [8]. More recently, real magnetic vdW materials having the *XY* and Heisenberg models have been studied to reveal data in good agreement with theories: $NiPS_3$ for *XY* model [9] and $MnPS_3$ for Heisenberg model [10].

Another interesting area of importance lies in the search for novel quantum phases with these magnetic vdW materials. For instance, when a long-range magnetic order is suppressed to occur at zero temperature by external variables like pressure, gating, field or doping it may lead to the emergence of novel phases near a so-called quantum critical point (QCP) [11]. This kind of physics has yet to be explored in a metallic 2D ferromagnetic vdW system. It is desirable that the transition temperature should be low enough that one can easily tune the transition temperature with, for example, a reasonably accessible pressure range, and without major perturbation to the system. The only metallic ferromagnetic vdW material reported so far is Fe_3GeTe_2 (FGT), which additionally exhibits a rich competition of magnetic phases [12]. With an anomalously high Curie temperature around 200 K, work has focused on pushing the transition temperature above room temperature [13]. Another interesting point to note on Fe_3GeTe_2 is the discovery of a topological nodal line in this system [14].

Despite these attractive properties of Fe_3GeTe_2, our preliminary results, along with recently published work [15] suggest that it needs an impractically high pressure to bring down the Curie temperature sufficiently to reach the quantum critical regime. We therefore aim to uncover a new system with a significantly lower Curie temperature and more accessible QCP. Here we need to note that although it is known that Fe deficiency tends to reduce the Curie point in FGT [16, 17] it suffers from one unavoidable problem; the ferromagnetic transition becomes broadened by the chemical inhomogeneity.

In this work we report the synthesis of single crystals of $(Fe,Co)_3GeTe_2$, and show this new material to address both problems described in undoped FGT and to potentially lead to new physics questions. Firstly, Co-doping suppresses the
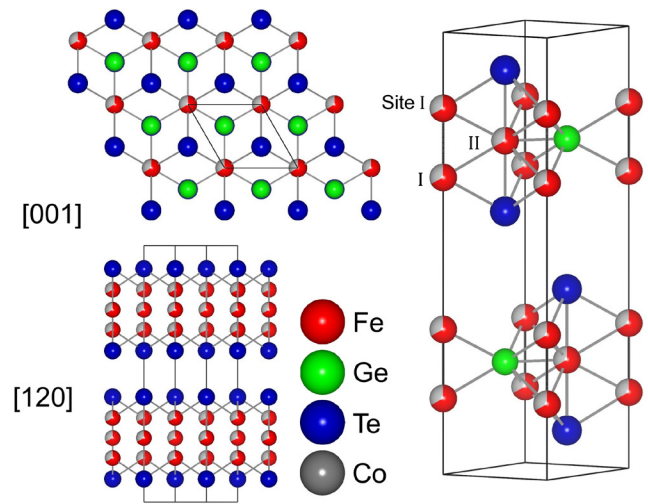

Figure 1. Crystal structure of $Fe_2Co_{0.7}GeTe_2$. It belongs to the $P6_3/mmc$ space group—the same as Fe_3GeTe_2. The lattice parameters are $a = 3.99$ Å, $c = 16.34$ Å. Co atoms are distributed randomly around the possible Fe sites. The volume fraction in the red/grey colored ball reflects the occupancy of iron and cobalt atoms in the sites.

Curie temperature to less than 50 K, which makes the pressure-tuned QCP potentially within the reach of a few-GPa range. Secondly, of importance to QCP physics, the transition of $(Fe,Co)_3GeTe_2$ remains as sharp as in FGT, indicating that there is less of an issue of stoichiometry than with our deficient FGT samples. Thirdly, we show a significant increase in the coercivity over that of $Fe_{3-x}GeTe_2$, which we attribute to the higher Hund coupling of the Co atom. These properties of our $(Fe,Co)_3GeTe_2$ single crystal open up the possibility of a quantum phase transition in a 2D metallic ferromagnet, and further exploration of low-dimensional magnetism and devices.

2. Experimental details

To synthesize single crystalline $(Fe,Co)_3GeTe_2$, Fe powder (99.998%, Alfa Aesar), Co powder (99.998%, Alfa Aesar), Ge powder (99.99%, Aldrich) and Te powder (99.999%, Alfa Aesar) totaling 0.5 g were mixed in a stoichiometric ratio in an Ar atmosphere glove box. The mixture was sealed in an evacuated quartz tube with an added 5 mg cm^{-3} I_2 flux agent. The quartz tubes were then heated to 750 °C/700 °C at a slow heating rate of 2 °C min^{-1} within a two-zone furnace and then held at these temperatures for 1 week. They were then slowly cooled to room temperature over 12 h, after which black shiny platelet flakes were found formed in the cold-temperature zone. For the purpose of comparison, we also prepared $Fe_{3-x}GeTe_2$ single crystals using the same method.

To check the quality and crystallinity of the resulting materials, we used both energy dispersive x-ray spectroscopy (EDX, EDS) and powder x-ray diffraction (XRD). To further confirm the vdW layered structure of $(Fe,Co)_3GeTe_2$, we employed the cross-sectional transmission electron microscope (TEM) analysis of $(Fe,Co)_3GeTe_2$ using a probe-Cs-corrected Titan^3 microscope (FEI) equipped with a Super-X^{TM}
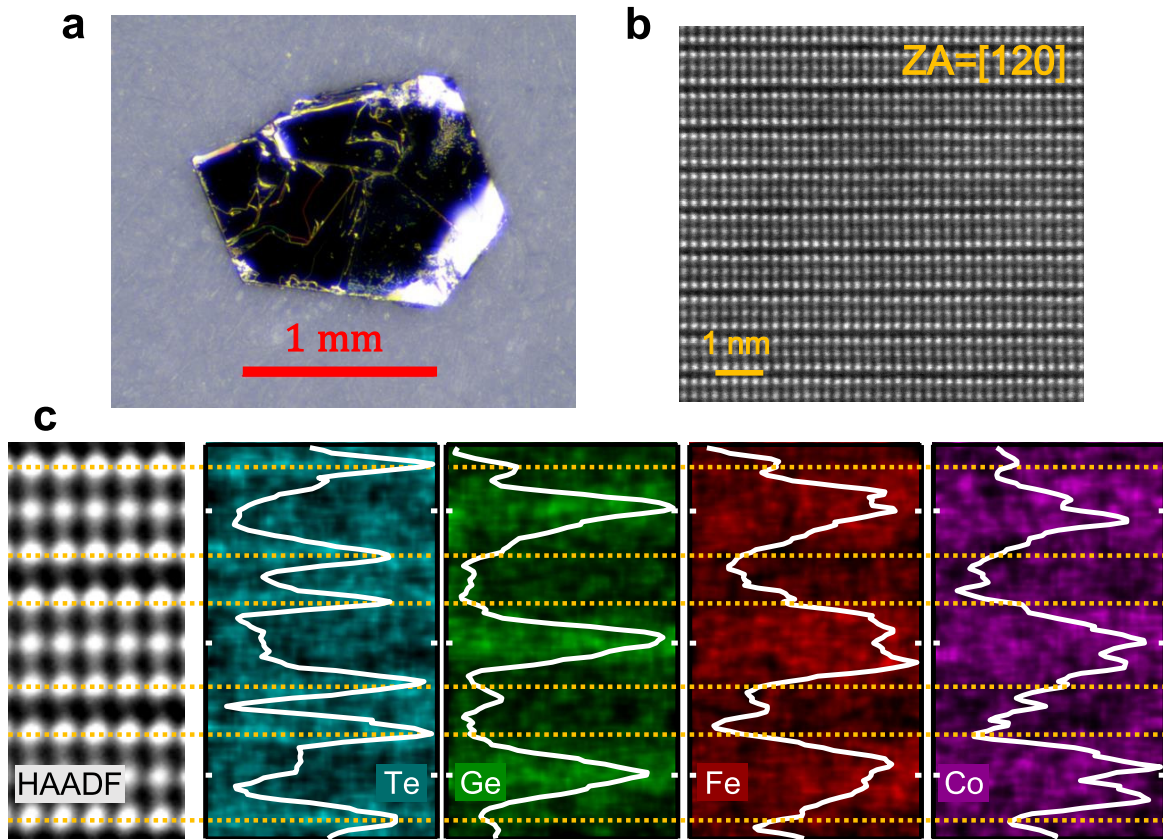
Figure 2. (a) Photograph of a $Fe_2Co_{0.7}GeTe_2$ crystal. (b) HAADF STEM image of $Fe_2Co_{0.7}GeTe_2$. vdW layers lie between the Te columns, the black-striped areas between the brightest spots in the image. (c) Energy dispersive x-ray spectroscopy normalized intensity maps in the HAADF image. The inset graphs show the normalized intensity line profile of corresponding atoms along the crystal planes. The intensities of the EDX signals from Fe and Co indicate that Co atoms occupy the Fe sites I and II randomly.

EDS detector at an accelerating voltage of 300 keV. To avoid the knock-on damage of the *e*-beam, an *e*-beam current less than 70 pA was used for imaging and EDX analysis. TEM samples were prepared by focused ion beam (FIB, Helios Nanolab 450F1, FEI) at 5 keV for slice milling and 2 keV for removing Ga-induced surface damage layer, respectively.

The magnetic property measurements were done using a Quantum Design MPMS3 EverCool SQUID magnetometer with vibrating-sample-magnetometer option. Heat capacity measurements were carried out using a Quantum Design PPMS cryostat and resistivity measurements were done using a Keithley 6430 source meter with current excitation in the standard four-wire geometry and a closed-cycle cryostat system developed in-house. These resistivity measurements were carried out in the *ab*-plane of bulk single crystals. Crystal dimensions were characterized by inspection under microscope. To cleave the single crystal into few-/mono-layer thickness, we used the mechanical exfoliation method onto a Au evaporated substrate [18] inside an Ar atmosphere glove box. To characterize the thickness and topography of cleaved samples we used a Park Systems NX10 atomic force microscope installed inside the glove box.

Our scanning tunneling microscope (STM) measurements were performed using the Unisoku low-temperature STM at 2.8 K with base pressure of $<1 \times 10^{-10}$ Torr. Prior to the STM measurement, our mechanically cut Pt/Ir tips were
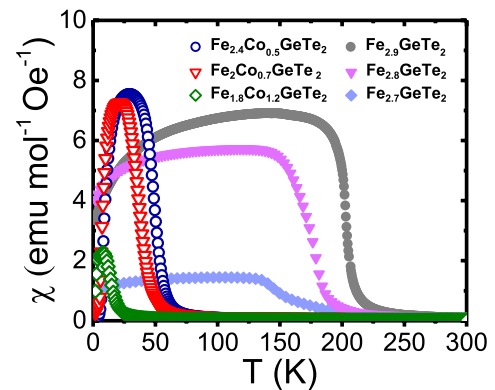

Figure 3. Zero-field cooling curve of temperature-dependent molar susceptibility for $Fe_{3-x}GeTe_2$ and $(Fe,Co)_{3-x}GeTe_2$ with 500 Oe of magnetic field applied along the *c*-axis. For $(Fe,Co)_{3-x}GeTe_2$, the transition temperatures are suppressed as compared to $Fe_{3-x}GeTe_2$, but it still shows a clean transition below 51 K ($Fe_{2.4}Co_{0.5}GeTe_2$), 37 K ($Fe_2Co_{0.7}GeTe_2$), and 14 K ($Fe_{1.8}Co_{1.2}GeTe_2$).

carefully characterized on Ag(1 1 1) [19]. We first measured the Ag(1 1 1) surface and checked the Ag(1 1 1) surface state. The Ag(1 1 1) substrate was cleaned over several cycles of Ar^+ ion sputtering and annealing in an ultrahigh vacuum chamber. Then, after $(Fe,Co)_3GeTe_2$ samples were cleaved several times using Scotch tape, the samples were transferred to the STM load-lock chamber. Final cleavage was performed at a
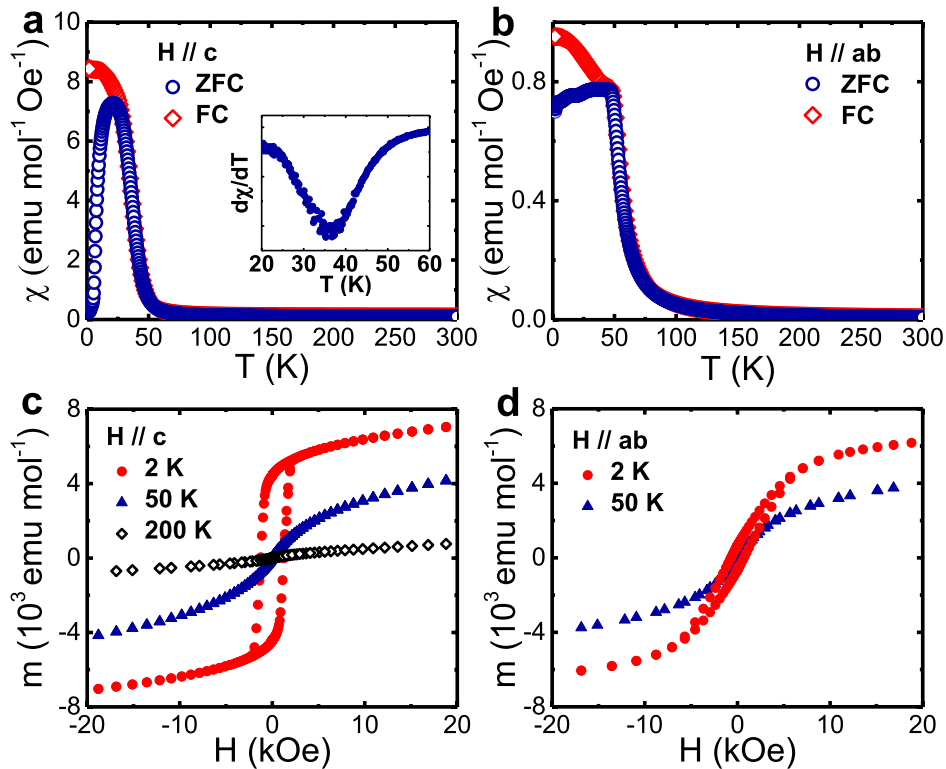
Figure 4. (a) and (b) Temperature-dependent molar susceptibility, measured with 500 Oe. The magnetic easy axis is along the *c*-axis. Inset in (a) is a first derivative of $M(T)$ curve used to extract the value of T_C. The local minimum in the graph implies $T_C = 37$ K for $Fe_2Co_{0.7}GeTe_2$. (c) and (d) M(H) curve from -2 T to 2 T at 2, 50, and 200 K with the magnetic field perpendicular (c) to and within (d) the crystal planes. The measured value of H_C was 1.85 kOe at 2 K, which is an order of magnitude higher than that of Fe deficient $Fe_{3-x}GeTe_2$.

low pressure of ~1×10^{-8} Torr in the load-lock chamber, and the sample was immediately inserted into the STM head to keep the surface as fresh as possible. During all our measurements, we monitored the sample surface with minimal noticeable changes in the sample quality.

3. Results and discussion

Single crystals $(Fe,Co)_3GeTe_2$ with several Fe to Co ratios including $Fe_2Co_{0.7}GeTe_2$ were formed in the cold temperature region of the furnace with a typical crystal size of $2 \times 2 \times 0.3$ mm^3 and a reflective dark grey coloring. Our subsequent XRD data show no change in the crystal structure for all our samples and the homogeneous mixing between Fe and Co was further determined by TEM analysis as shown in figure 1 (see also figure 2). It was found to form the same space group as FGT, P6$_3$/mmc, but Co atoms locate randomly on both Fe sites in the FGT structure. To clarify the crystal structure, a high-angle annular dark field scanning transmission electron microscope (HAADF STEM) image along the [1 2 0] crystal direction is shown in figure 2(b). The heavier atoms are the brighter, thus the transition metals are less visible than Te and Ge in this figure. The layered atomic arrangement and a vdW gap are clearly visible in the image. To see whether Co atoms prefer some sites, we extracted energy dispersive x-ray spectroscopy (EDX) normalized intensity maps from the TEM imaging showing the atomic distributions presented in figure 2(c). EDX mapping shows the atomic distribution

along the crystallographic *c* axis, and the peaks correspond to the atomic sites Te–Fe/Co (site I)—Ge/Fe/Co (site II)—Fe/Co (site I)—Te in each layer. From this we conclude that Co has no preference on the possible transition metal sites and is distributed randomly and uniformly. These images and maps additionally demonstrate the clean single-crystal nature of the sample, despite the weak inter-layer interactions.

Figure 3 shows the result of temperature-dependent magnetization measurements for several samples: three of $Fe_{3-x}GeTe_2$ and three of $(Fe,Co)_3GeTe_2$ with different stoichiometries. As in FGT, $(Fe,Co)_3GeTe_2$ exhibits ferromagnetic ordering clearly visible from the sharp upturn due to spontaneous magnetization below T_C in the magnetization data. The values of T_C are significantly suppressed in $(Fe,Co)_3GeTe_2$ as compared to undoped FGT even in the Fe-deficient case. A similar suppression of T_C was reported in a previous Ni doping study [17], but the ferromagnetic transition becomes visibly broadened with doping. This latter observation is in sharp contrast with our observation of the transition temperature remaining as sharp in $(Fe,Co)_3GeTe_2$ as in undoped Fe_3GeTe_2.

To make our case clearer, we show the temperature-dependent magnetization for $Fe_2Co_{0.7}GeTe_2$ in figures 4(a) and (b). It has a ferromagnetic ground state below a Curie temperature $T_C = 37$ (2) K. As compared with the undoped FGT sample, a stronger anisotropy is also observed in the $M(H)$ curves (with the *c*-axis magnetic forming the easy axis). From the strong anisotropy induced by Co doping, we can expect the ferromagnetic order to easily survive down to a monolayer

thickness, but verification of this awaits further study. A difference between field-cooled cooling and warming magnetization curves is observed in FGT along the *c*-axis. That difference stems from the interlayer antiferromagnetic coupling, which competes with the ferromagnetic state [20]. However, in the Co-doped system, particularly in $Fe_2Co_{0.7}GeTe_2$, there is no visible difference observed between the field-cooled cooling and warming curves along either the *c*-axis or *ab*-plane: further evidence of a strong ferromagnetic system—but with a lower ordering temperature.

Field-dependent magnetization data show clear ferromagnetic hysteresis loops (see figures 4(c) and (d)). As temperature approaches T_C the hysteresis loops shrink, and above T_C the system reverts to paramagnetic behavior—linear inverse susceptibility. Despite the atomic disorder that attributes to the dilution of magnetic properties, the coercive field was found to be enhanced to a value of 1.85 ± 0.1 kOe at 2 K. The value is an order of magnitude larger than the value of 200 Oe observed in the Fe-deficient bulk FGT system [16, 21]—despite the lower ordering temperature. In some vdW layered systems including CrI_3 and Fe_3GeTe_2 [8, 21], H_c becomes larger as the layer number shrinks—we can then expect much harder ferromagnetism in few-layer samples of $(Fe,Co)_3GeTe_2$. There are only a few materials classified as hard vdW ferromagnets in the bulk system [22, 23]—all but FGT are insulators. $(Fe,Co)_3GeTe_2$ forms an alternative ferromagnetic vdW metal, with many similarities but also key differences to FGT.

The saturation moment was found to be 1.1 (3) μ_B/f.u. at 2 K in $Fe_2Co_{0.7}GeTe_2$. From the inverse susceptibility, we estimated a Curie–Weiss temperature of $\theta_{CW} = 39.5$ (2) K, and effective moment 3.39 (8) μ_B/TM atoms. In this system, the effective moment is smaller than in the FGT system and the saturation moment is about one-third compared to that of undoped FGT [24]. A similar reduction in moment values was also reported in the Ni doping study [17]. From the moments above, we calculated the Rhodes-Wohlfarth ratio p_c/p_s in $Fe_2Co_{0.7}GeTe_2$ to verify that the Co-doped system satisfies the Stoner model. From $p_c (p_c + 2) \equiv p_{eff}^2$, and the saturation moment p_s obtained from magnetization data, the ratio p_c/p_s was calculated to be 2.3 for $Fe_2Co_{0.7}GeTe_2$. It is smaller than the values for FGT [16, 24], but still deviates significantly from $p_c/p_s = 1$, which indicates the spin system in Co-doped FGT as itinerant nature—a localized description for the spin system in Co-doped FGT is not adequate.

We find that the transport properties of $(Fe,Co)_3GeTe_2$ show similar behavior to those of FGT [24]. For electron transport $(Fe,Co)_3GeTe_2$ also shows metallic conduction in the temperature-dependent in-plane resistivity data—the resistance decreasing with decreasing temperature. Like FGT, a kink is seen at the ferromagnetic transition temperature as shown in figure 5(a) and a resistivity upturn is additionally observed below 30 K. In order to explore the thermodynamic origin of this anomaly, we measured heat capacity data as shown in figure 5(b): which shows a peak at 37 K, corresponding to the Curie temperature found from the magnetization. The heat capacity data were fitted to a low temperature approximation of the Debye formula:
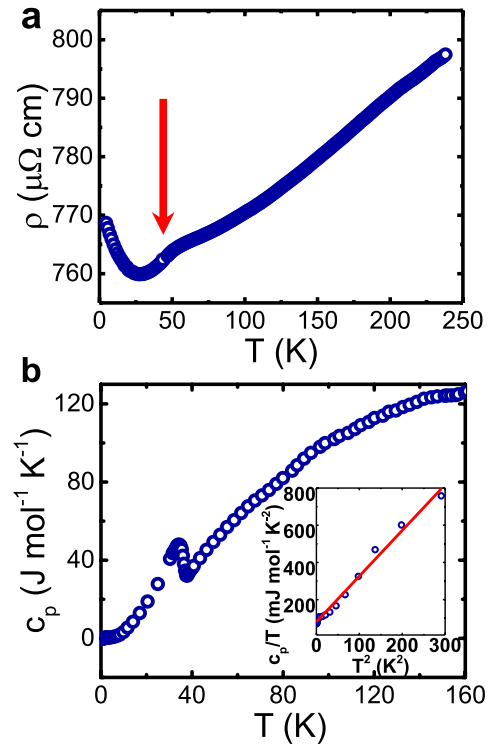

Figure 5. (a) Temperature dependence of in-plane electrical resistivity. The arrow indicates the kink at T_c. As in FGT, a resistivity minimum appears below 25 K with an overall metallic behavior for $Fe_2Co_{0.7}GeTe_2$. (b) Heat capacity data of $Fe_2Co_{0.7}GeTe_2$ show a peak at 37 K, which corresponds to the Curie temperature. Inset shows approximated Debye fitting, $Cp/T = \gamma + \beta T^2$, where $\gamma = 85$ mJ mol^{-1} K^{-1}, $\beta = 2.46$ mJ mol^{-1} K^{-4}.

$$Cp/T = \gamma + \beta T^2.$$

Values of $\gamma = 85$ (3) mJ mol^{-1} K^{-1}, and $\beta = 2.46$ (5) mJ mol^{-1} K^{-4} were found for the Sommerfeld electronic specific heat coefficient and the low-temperature limit of the phonon contribution to the heat capacity. This yields the Debye temperature $\Theta_D = 168$ (2) K. The coefficients are comparable to the ones found in FGT, and as in FGT, spin fluctuations strongly contribute to γ [24]. It is also important to note that the large γ also seems to be only weakly affected by doping: it is a good indication of significant correlation already present in the sample and not destroyed by doping. These results indicate that Co doping in FGT does modulate the magnetic properties but does not strongly modify the electronic properties.

In order to demonstrate the vdW nature of the crystal lattice, we have performed mechanical exfoliation to produce monolayers of $Fe_2Co_{0.7}GeTe_2$ crystals as shown in figures 6(a) and (b). From the measured AFM line profiles we can find monolayer samples (thickness half of the *c* crystal axis) with a typical size of a few microns and 1 nm thick, including an inevitable slight offset about 0.2 nm from the substrate to the flakes. Due to low optical contrast, a single layer of $Fe_2Co_{0.7}GeTe_2$ is rather difficult to see on top of the Au substrate. As with FGT, thin samples were found to be highly air-sensitive and had to be handled in an inert atmosphere.
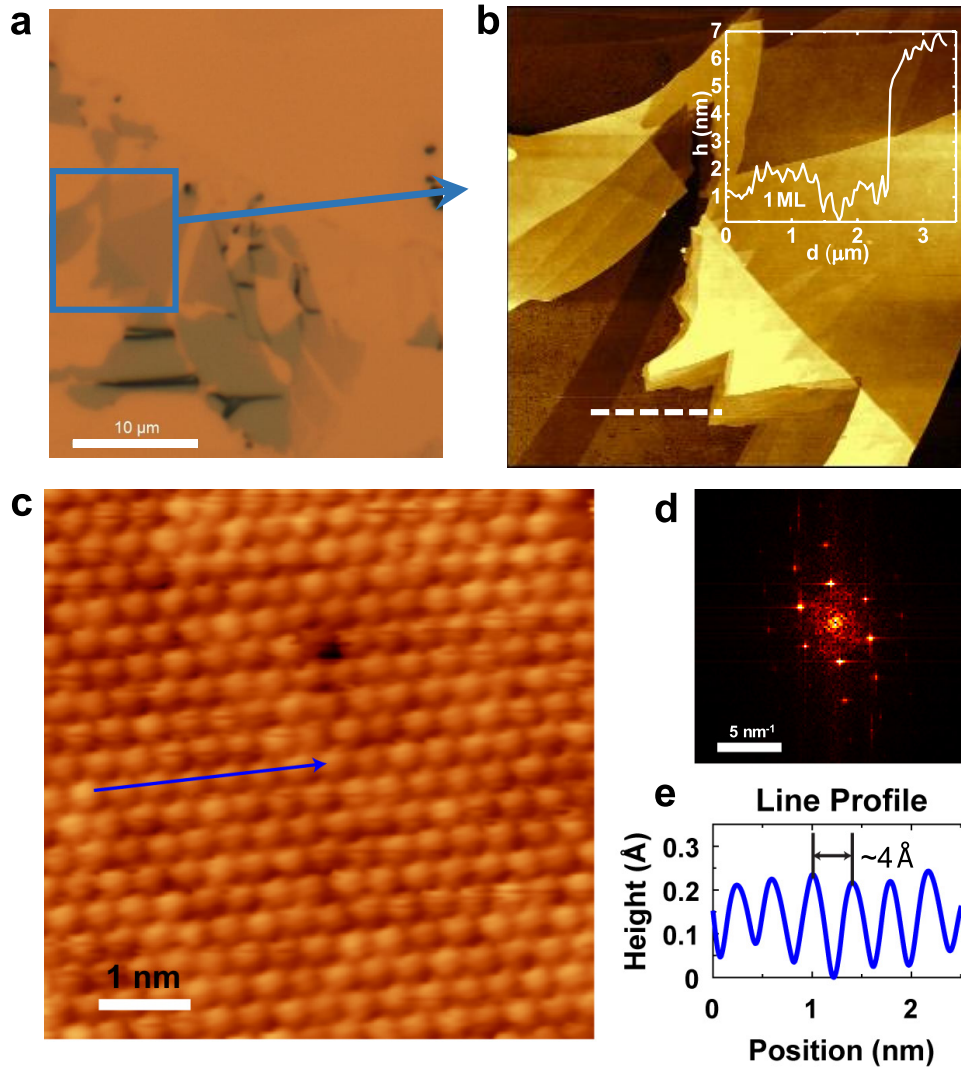
Figure 6. (a) Optical image of exfoliated $Fe_2Co_{0.7}GeTe_2$ on Au 15 nm substrate. (b) AFM topographical image of boxed area in (a). The inset graph is the thickness profile along the white dashed line, which shows that our sample is exfoliated down to the thickness of 1 nm, corresponding to a monolayer. (c) STM topograph of $Fe_2Co_{0.7}GeTe_2$ at atomic resolution ($V_s = -400$ mV, and $I_t = 0.5$ nA) and (d) its Fourier transform. (e) Line profile along the blue arrow in the STM topograph.

Figures 6(c)–(e) shows a high-resolution STM topograph image of a $Fe_2Co_{0.7}GeTe_2$ surface, which displays a well-crystallized triangular lattice structure. The bright protrusions are Te atoms: cleaving occurred at the Te–Te interface. We found that the lattice constant of the $Fe_2Co_{0.7}GeTe_2$ surface was ~4 Å through the line profile shown in the figure and the Fourier transform of the topograph image, which agree well with the lattice parameter a in the crystal structure. We have demonstrated that Co-substituted FGT is cleavable down to monolayer thickness.

4. Conclusion

We have reported the synthesis, characterization and measurements of bulk properties of metallic vdW ferromagnet Co-doped Fe_3GeTe_2, $(Fe,Co)_3GeTe_2$ using a wide variety of experimental techniques. This system shows metallic behavior and ferromagnetism below the Curie temperature, whose value depends on the doping concentration of Co. Although

the Curie temperature is suppressed significantly with Co doping, the transition remains as sharp as in the undoped case. It is in marked contrast to the case of Ni doping [17], which reduces the transition temperature quite rapidly and eventually leads to a cluster glass phase. These distinct features of the ferromagnetism found in the $(Fe,Co)_3GeTe_2$ systems, with the many advantages of FGT such as electronic properties suggest that it can be a reliable candidate as a platform for the exploration of 2D magnetism in the true 2D limit and potential quantum critical physics. The drastically lowered transition temperature and clean nature of the tuning place this material within the accessible range of a possible critical point through methods such as hydrostatic pressure. The sharpness of the transition, the random distribution of dopants, and the robustness of the heat capacity coefficients all show this doping method to be a clean tuning of the magnetic properties of the system, while leaving the structural and electronic states intact. The fact that this material, like FGT, is metallic means that transport measurements can be carried out, on arbitrarily

small and thin samples, under pressure or gating, and the magnetic properties ascertained from these—in contrast to all other existing vdW ferromagnets. We have demonstrated this sample to be cleavable down to monolayer thickness; an investigation into the evolution of the magnetism as this true 2D limit is approached is a clear next direction for research into these materials.

Acknowledgments

Note to be added

While preparing this work, we came across one recent publication [25] reporting on Co-doped Fe_3GeTe_2 with a different focus. They were more interested in the domain pinning effects in their samples.

ORCID iDs

Youngtek Oh ⬚ https://orcid.org/0000-0002-2791-4545
Je-Geun Park ⬚ https://orcid.org/0000-0002-3930-4226

References

[1] Berezinskii V L 1971 *Sov. Phys. JETP* **32** 493–500
[2] Kosterlitz J M and Thouless D J 1973 *J. Phys. C: Solid State Phys.* **6** 1181
[3] Park J-G 2016 *J. Phys.: Condens. Matter* **28** 301001
[4] Burch K S, Mandrus D and Park J-G 2018 *Nature* **563** 47
[5] Onsager L 1944 *Phys. Rev.* **65** 117
[6] Lee J-U, Lee S, Ryoo J H, Kang S, Kim T Y, Kim P, Park C-H, Park J-G and Cheong H 2016 *Nano Lett.* **16** 7433–8
[7] Gong C *et al* 2017 *Nature* **546** 265–9
[8] Huang B *et al* 2017 *Nature* **546** 270–3
[9] Kim K, Lim S Y, Lee J-U, Lee S, Kim T Y, Park K, Jeon G S, Park C-H, Park J-G and Cheong H 2019 *Nat. Commun.* **10** 345
[10] Kim K *et al* 2019 *2D Mater.* **6** 041001
[11] Saxena S S *et al* 2000 *Nature* **406** 587–92
[12] Deiseroth H-J, Aleksandrov K, Reiner C, Kienle L and Kremer R K 2006 *Eur. J. Inorg. Chem.* **37** 1561–7
[13] Deng Y *et al* 2018 *Nature* **563** 94–9
[14] Kim K *et al* 2018 *Nat. Mater.* **17** 794–9
[15] Wang X *et al* 2019 *Phys. Rev.* B **100** 014407
[16] May A F, Calder S, Cantoni C, Cao H and Mcguire M A 2016 *Phys. Rev.* B **93** 014411
[17] Drachuck G, Salman Z, Masters M W, Taufour V, Lamichhane T N, Lin Q, Straszheim W E, Bud'ko S L and Canfield P C 2018 *Phys. Rev.* B **98** 144434
[18] Fei Z *et al* 2018 *Nat. Mater.* **17** 778–824
[19] Oh Y, Lee J, Park J, Kwon H, Jeon I, Kim S W, Kim G, Park S and Hwang S W 2018 *2D Mater.* **5** 035005
[20] Yi J, Zhuang H, Zou Q, Wu Z, Cao G, Tang S, Calder S A, Kent P R C, Mandrus D and Gai Z 2016 *2D Mater.* **4** 011005
[21] Tan C, Lee J, Jung S-G, Park T, Albarakati S, Partridge J, Field M R, McCulloch D G, Wang L and Lee C 2018 *Nat. Commun.* **9** 1554
[22] Son S *et al* 2019 *Phys. Rev.* B **99** 041402
[23] Kong T, Stolze K, Timmons E I, Tao J, Ni D, Guo S, Yang Z, Prozorov R and Cava R J 2019 *Adv. Mater.* **31** 1808074
[24] Chen B, Yang J, Wang H, Imai M, Ohta H, Michioka C, Yoshimura K and Fang M 2013 *J. Phys. Soc. Japan* **82** 124711
[25] Tian C, Wang C, Ji W, Wang J, Xia T, Wang L, Liu J, Zhang H and Cheng P 2019 *Phys. Rev.* B **99** 184428